JOM, Vol. 69, No. 11, 2017
DOI: 10.1007/s11837-017-2523-3


# The Role of Compositional Tuning of the Distributed Exchange on Magnetocaloric Properties of High-Entropy Alloys

ALICE PERRIN,[1,3] MONICA SORESCU,[2] MARI-THERESE BURTON,[1] DAVID E. LAUGHLIN,[1] and MICHAEL MCHENRY[1]

1.—Department of Materials Science and Engineering, Carnegie Mellon Univeristy, Pittsburgh, PA 15213, USA. 2.—Department of Physics, Duquesne University, Pittsburgh, PA 15282, USA. 3.—e-mail: aperrin@andrew.cmu.edu

This paper explores the FeCoNiCuMn high-entropy alloy system, where small departures from equiatomic composition have yielded technologically interesting 300-K Curie temperatures ($T_c$), making them promising for magnetocaloric applications. We also demonstrate that the small deviations from equiatomic compositions do not affect the structural stability of our single-phase fcc-based solid solutions. Room-temperature Mössbauer spectroscopy measurements provide evidence for the distributed exchange interactions ($J_{ex}$) occurring between the magnetic elements, which contribute to a broadened magnetocaloric effect observed for these alloys. The average hyperfine field observed in the Mössbauer spectra decreases as the $T_c$ of the alloys decrease, confirming direct current magnetic measurements. Multiple peaks in the hyperfine field distribution are interpreted considering pairwise ferromagnetic or antiferromagnetic $J_{ex}$ between all elements except the Cu diluent as contributing to overall magnetic exchange in the alloy.

## INTRODUCTION

Magnetocaloric refrigeration offers more energy efficiency, by 20%, than conventional gas compression refrigeration, and has the additional advantage of being environmentally friendly because ozone depleting and warming refrigerants are not used.[1,2] Critical rare earth metals (REs) and compounds have been studied because of their large magnetocaloric response and working temperatures close to room temperature (RT).[3–5] However, the scarcity, high price and corrosion of REs limit their commercial use, so more sustainable transition metal-based alloys have been investigated to replace them.[6] Outside of commercial refrigeration, magnetocaloric materials have been explored for use in active cooling of motors in the form of ferrofluids.[7,8]

Magnetocaloric materials fall into two classes based on: (1) first-order magneto-structural phase transitions (FOMPs) and (2) second-order magnetic transitions. The first type, giant magnetocaloric effect materials, exhibit a large and narrow peak magnetic entropy change accompanying a magneto-structural phase transition. A large peak entropy change is often accompanied by undesirable thermal hysteresis[3,4,9] and requires staging of materials with different $T_c$'s to span a relevant thermodynamic cycle. Materials with a seconnd-order magnetic phase transition usually show a lower peak entropy change, but a broader peak results in an enhanced refrigerant capacity.[10,11] These materials have reduced hysteresis loss and tunable Curie temperature, $T_c$.[12,13] Optimum materials possess features of each class: (1) large peak entropy change, (2) large refrigerant capacity, (3) limited thermal hysteresis and (4) resistance to thermomechanical fatigue.

We are assessing high-entropy alloys (HEAs) to determine their applicability as magnetocaloric materials. These multicomponent alloys undergo second-order magnetic transitions, which are broadened through compositional disorder-derived distributed exchange interactions.[14–17] They are of interest because their multicomponent nature allows $T_c$ tuning and control of the refrigeration capacity through the breadth of the second-order transition. Broadening due to random distribution of magnetic atoms on an fcc lattice[18] is less than the resulting broadening from positional disorder-derived distributions previously observed in Ni-Fe-

(Published online August 16, 2017)

based amorphous alloys.[19] Extensive work has already been carried out in calculating magnetic properties of HEAs alloys using ab initio calculations in the framework of density functional theory,[20–23] but experimental exploration of high-entropy alloy systems for magnetocaloric response have been more limited.

### The Magnetocaloric Effect (MCE)

The magnetocaloric effect (MCE) is measured by the temperature change a magnetic material experiences as it enters or leaves a magnetic field adiabatically. This occurs because the magnetic entropy ($\Delta S$) of the system decreases upon application of a magnetic field. In order for the total entropy change to remain zero, the thermal entropy of the system increases, causing an increase in the temperature of the system. The opposite occurs when the field is removed, and we can quantify the change in thermal entropy by indirectly measuring the magnetic entropy change, which is defined as:

$$\Delta S_M = \int_0^{H_{\max}} \left(\frac{\partial M}{\partial T}\right)_H \mathrm{d}H \qquad (1)$$

Using Eq. 1, we can integrate isothermal magnetization versus field curves taken over a range of temperatures to solve for the change in magnetic entropy, $\Delta S_M$ with temperature.[24] A common figure-of-merit for comparing magnetocaloric materials is the refrigeration capacity (RC) which takes into account both the temperature range and the magnitude of entropy change for a given material. RC can be measured many ways, but a common definition is the peak entropy multiplied by the temperature span at the full width, half maximum (FWHM) of the entropy curve:

$$\mathrm{RC}_{FWHM} = |\Delta S_M \Delta T_{FWHM}| \qquad (2)$$

The value of the peak entropy and the corresponding RC scale with the applied field, and the temperature at which the peak entropy occurs also increases with increasing applied fields.[25]

Another figure-of-merit for determining the commercial viability of a magnetocaloric material is the temperature change over one cycle at the peak entropy change can be approximated as:

$$\Delta T_{ad} = -\left(\frac{T}{C_p}\right)|\Delta S_{\max}| \qquad (3)$$

This value gives us an upper limit on the temperature change possible to achieve in one magnetocaloric cycle.

### High-Entropy Alloys

HEAs are alloys containing 5+ components in relatively equiatomic amounts (5–35% of each[26]) to increase the configurational entropy of the system ($S_{config} = R\sum_i X_i \ln(X_i)$).

In a HEA, the mixing entropy balances the mixing enthalpy and allows for the formation of a solid solution, which is a uniform, random distribution of elements on a crystal lattice.[27] However, it is thought that lattice distortion caused by the different atomic sizes of the constituents also contributes to the phase stability[28] HEAs have been studied for the past few decades for structural applications due to their attractive mechanical properties and structural advances, but more recently have been identified as potential candidates for new magnetocaloric materials because the random distribution of several elements on a crystal lattice results in exchange interactions between each magnetic element present. The presence of several different exchange interactions broadens the temperature range over which we see a significant magnetocaloric response.

Several groups have characterized the four-component HEA FeCoNiCr.[29–31] Lucas et al.[32] characterized the magnetic behavior of $\mathrm{FeCoNiCrPd}_x$ for $0 \leq x \leq 2$. Kurniawan et al.[33] characterized several HEAs of the form FeCoNiCu$X$ where $X$ = Mn, Pt, Ag, and Mo and found equiatomic FeCoNiCuMn to be the most promising candidate for further study given its low $T_c$ (400 K). This work explores the FeCoNiCuMn alloy system through slight compositional variation and identifies two alloys with RT magnetic transition ranges and nearly equivalent RCs.

## EXPERIMENTAL METHODS

Our alloys are produced in a two-step process. Ingots of the nominal compositions of each alloy are produced using high-purity bulk elemental samples in a Mini Arc Melting System MAM-1 (Edmund Buhler) in an inert argon atmosphere. They are then remelted several times to ensure homogeneous distribution of elements. These ingots are melt-spun using an SC Melt Spinner (Edmund Buhler) in a low-pressure argon environment on a copper quenching wheel with a circumferential speed of 40 m/s . Typically, this process results in continuous ribbons of metallic glass alloys, but the brittleness of these crystalline solid solutions instead results in irregular flakes of material.

To confirm that the alloys are single-phase solid solutions, we performed x-ray diffraction with a Philips X'Pert multipurpose diffractometer working in continuous scanning mode with CuK$\alpha$ radiation ($\lambda$ = 0.1541874 nm) to determine the crystal structure and lattice parameter of each sample. Lattice parameters were calculated using the Nelson–Riley method.[34] All magnetic measurements were taken with a Lakeshore Vibrating Sample Magnetometer attached to a Quantum Design Physical Properties Measurement System. Measurements of the heat capacity of our alloys were taken with a Perkin Elmer Differential Scanning Calorimeter (DSC). The slope of the measured heat flow versus

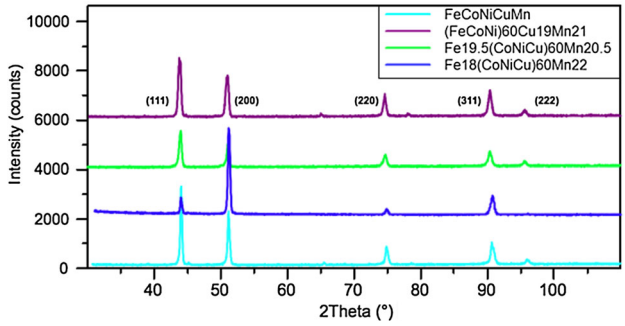


Fig. 1. X-ray diffraction peaks for three non-equiatomic alloys in the Fe-Mn and Cu-Mn pseudo-binaries compared with peaks for equiatomic FeCoNiCuMn (bottom). Peaks for the top scan are indexed and reveal a single-phase, fcc crystal structure; all other diffraction patterns shown are also clearly fcc and show little change in lattice parameter or peak broadness.

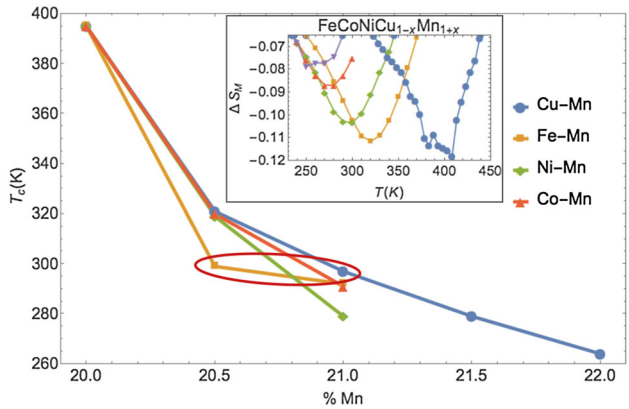


Fig. 2. $T_c$ versus Mn content for each set of pseudo-binary variations. The alloys with the largest RC at $T_c$ = 300 K are circled in red. Inset $\Delta S$ versus T for $FeCoNiCu_{1-x}Mn_{1+x}$ for $0 \leq x \leq 0.1$.

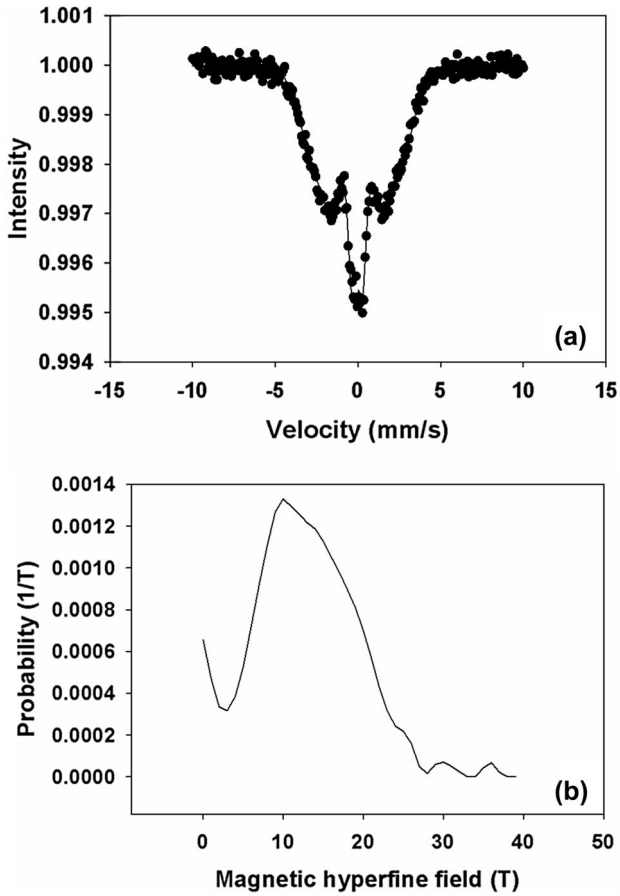


Fig. 3. RT transmission Mössbauer spectrum for FeCoNiCuMn (top) which corresponds with hyperfine magnetic field distribution (bottom).

temperature yields the heat capacity of the sample. All transmission Mössbauer spectroscopy was performed at RT with a 57Co(Rh) $\gamma$-ray source and a Ranger Scientific constant acceleration spectrometer.

## RESULTS AND DISCUSSION

### Compositional Variation

Previous work explored five-component, equiatomic HEAs of the form FeCoNiCu$X$ and found FeCoNiCuMn to be the most promising alloy for further study.[33] Iron, cobalt, and nickel have been chosen as ferromagnetic components to maximize configurational entropy while keeping the overall magnetization of each alloy large. The fourth component, copper, was added as a diamagnetic diluent, which served to decrease the $T_c$ of the alloys by decreasing the summed random exchange interactions but not affecting the strength of the pairwise ferromagnetic interactions. The fifth component of each alloy was chosen from transition metals with different types of exchange coupling to observe the effect of each on the magnetic and structural properties of the alloy. The addition of antiferromagnetic manganese, Mn, which contributes negative exchange interactions to the system, dramatically lowers $T_c$ of the alloy from over 1000 K to 400 K.

To further tune $T_c$ of alloys in the FeCoNiCuMn alloy system to achieve values even closer to RT, we studied several alloys in which the Mn content was varied in pseudo-binary alloys: $FeCoNiCu_{1-x}Mn_{1+x}$, $FeCoNi_{1-x}CuMn_{1+x}$, $FeCo_{1-x}NiCuMn_{1+x}$ and $Fe_{1-x}CoNiCuMn_{1+x}$. Each variation achieved a $T_c$ at RT with very small compositional changes ($x < 0.1$), and all alloys were confirmed to be single-phase, fcc solid solutions using x-ray diffraction (Fig. 1). Of these, the Cu-Mn and Fe-Mn pseudo-binaries yielded alloys with the largest RCs (Fig. 2). For the Cu-varied system, $FeCoNiCu_{0.95}Mn_{1.05}$ was the composition found to have an RT magnetic transition, with a RC of 13.5 J/kg at $H_{max} = 0.55$ T (this scales up to 36 J/kg at $H_{max} = 1.5$ T). The Fe-varied alloy with an RT Curie temperature was $Fe_{0.975}CoNiCuMn_{1.025}$ and a refrigeration capacity of 14.0 J/kg at 0.55 T (which scales to

**Table I. Compiled data for Cu-Mn and Fe-Mn pseudo-binaries**

| Composition | % Mn | $T$ {peak} (K) | $\lvert\Delta S_{max}\rvert$ (J/kgK) | $RC_{FWHM}$ at $H_{max}$ (J/kg) | Average hyperfine field ($T$) | Isomer shift (mm/s) |
|---|---|---|---|---|---|---|
| FeCoNiCuMn | 20 | 395 | 0.115 | 16.5 | 12.68 | −0.051 |
| $FeCoNiCu_{0.975}Mn_{1.025}$ | 20.5 | 321 | 0.094 | 15.3 | 6.68 | −0.056 |
| $FeCoNiCu_{0.95}Mn_{1.05}$ | 21 | 297 | 0.10 | 13.5 | 5.07 | −0.086 |
| $FeCoNiCu_{0.925}Mn_{1.075}$ | 21.5 | 279 | 0.084 | 12.2 | 3.73 | −0.09 |
| $FeCoNiCu_{0.9}Mn_{1.1}$ | 22 | 264 | 0.081 | 9.6 | 3.41 | −0.08 |
| FeCoNiCuMn | 20 | 395 | 0.115 | 16.5 | 12.68 | −0.051 |
| $Fe_{0.975}CoNiCuMn_{1.025}$ | 20.5 | 299 | 0.105 | 14.0 | 6.24 | −0.079 |
| $Fe_{0.95}CoNiCuMn_{1.05}$ | 21 | 292 | 0.071 | 10.0 | 4.43 | −0.09 |

*Left* Magnetocaloric figures of merit, *Right* Mossbauer spectroscopy data.

38 J/kg at 1.5 T). These RC values are too low for these alloys to be viable for commercial refrigeration, but the possibility of enhanced structural integrity due to cocktail effects could make these alloys attractive for active cooling applications in extreme environments. DSC measurements of these alloys yield heat capacities around 550 J/kgK. For $FeCoNiCu_{0.95}Mn_{1.05}$, Eq. 3 yields $\Delta T_{ad} = 1.7$ K for a single demagnetization cycle from a maximum field of 1.5 T. At $H_{max} = 1$ T, this drops to $\Delta T_{ad} = 1.2$ K, which is comparable to experimental values obtained for two well-studied magnetocaloric materials, La(Fe, $Co, Si)_{13}$ ($\Delta T_{ad} = 2.4$ K) and $La_{0.67}Ca_{0.26}Sr_{0.07}Mn_{1.04}O_3$ ($\Delta T_{ad} = 1.0$ K), in an active magnetic regenerator refrigerator.[35]

### Mössbauer Spectroscopy Measurements

The transmission Mössbauer spectrum is a superposition of singlets, doublets and sextets that need to be deconvoluted to obtain the Mössbauer parameters corresponding to the hyperfine interactions present in the sample.[36] The isomer shift (chemical shift) corresponds to the electric monopole interaction between the nuclear charge distribution and the potential generated by the electronic charge distribution penetrating the nucleus. As a result of this interaction, the nuclear energy level will be shifted by a very small amount, which is different for each nuclear state. The isomer shift can be readily computed from a Mössbauer spectrum as the distance of the resonance line from zero Doppler velocity. In our case, it can be seen (Table I) that the isomer shift decreases when the iron content in the alloy increases. The quadrupole shift is a measure of the asymmetry of a sextet, while the sextet itself reflects the magnetic hyperfine interaction, which corresponds to the interaction between the magnetic dipole moment of the nucleus and the magnetic hyperfine field at the nuclear site. This hyperfine field can be thought of as the effective magnetic field acting at the location of the nucleus. When the hyperfine parameters fluctuate from one site to another, they give rise to hyperfine magnetic field distributions. The average value of this distribution can be studied as a function of the alloy composition (Fig. 3a and b). The average hyperfine field gives us a measure of the strength of the average magnetic response of an alloy, and the presence and absence of these hyperfine fields distinguishes the ferromagnetic and paramagnetic phases.

Both Cu-Mn and Fe-Mn pseudo-binaries produce a range of alloys with $T_c$ spanning from 400 K to below RT, and the average hyperfine field of these alloys decreased linearly with $T_c$ (Table I). However, it is still non-zero for the compositions with $T_c$ lower than RT, confirming that our materials undergo a broad, second-order magnetic transition. From hyperfine field distributions, we observe distinct peaks suggestive of the presence of exchange interactions of varying strength. Given that these alloys contain six distinct ferromagnetic exchange bonds (Fe-Fe, Fe-Co, Fe-Ni, Co-Co, Co-Ni, Ni-Ni), we postulate that this peak structure reflects the random distribution of these pairwise interactions in the alloy. These summed interactions contribute to the overall magnetic exchange and are likely responsible for the broad magnetocaloric response observed in these alloys. A quantitative model of the hyperfine field distribution will be the subject of future work.

## CONCLUSION

We explored several pseudo-binary compositional variations in the FeCoNiCuMn high-entropy alloy system and identified two alloys, $FeCoNiCu_{0.95}Mn_{1.05}$ and $Fe_{0.975}CoNiCuMn_{1.025}$ with $T_c$ near 300 K and RCs around 37 J/kg at maximum fields of 1.5 T. X-ray diffraction confirmed the single-phase, fcc crystallography of each alloy. The relative stability and structural integrity of these alloys make them attractive for use in extreme environments and active cooling despite their relatively low RC values. Mössbauer spectroscopy measurements made at RT qualitatively confirm the shift in the

alloys' peak magnetocaloric transition temperature as Mn content is increased, and the hyperfine field distributions obtained from the Mössbauer spectra contain multiple distinct peaks, giving evidence for the multiple pairwise ferromagnetic and antiferromagnetic interactions between the elements in these alloys.

## ACKNOWLEDGEMENTS

The authors acknowledge support from the National Science Foundation (NSF) through Grant DMR-1709247. The authors also acknowledge use of the Materials Characterization Facility at Carnegie Mellon University supported by Grant MCF-677785. We thank Vladimir Keylin and William Hasley III for sample preparation and assistance.

## REFERENCES

1. G.A. Schneidner Jr. and V.K. Pecharsky. *Ann. Rev. Mater. Sci.* 30, 387 (2000).
2. E. Brück, O. Tegus, L. Zhang, X.W. Li, F.R. de Boer, and K.H.J. Buschow. *J. Alloys Compd.* 383, 32 (2004).
3. V.K. Pecharsky and G.A. Schneidner Jr. *Phys. Rev. Lett.* 78, 4494 (1997).
4. V. Provenzano, A.J. Shapiro, and R.D. Shull. *Nature* 429, 853 (2004).
5. N. Carsen, R. Fingers, M.E. McHenry, D. Chaumette, and L. Alger. Unclassified NATO Report, Washington (2015).
6. O. Tegus, E. Brück, K.H.J. Buschow, and F.R. de Boer. *Nature* 415, 150 (2002).
7. V. Chaudhary and R. Ramanujan. *Sci. Rep.* 6, 35156 (2016).
8. J. Lawa, V. Francoc, P. Keblinski, and R. Ramanujana. *Appl. Therm. Eng.* 52, 17 (2012).
9. T. Krenke, E. Duman, M. Acet, E.F. Wassermann, X. Moya, L. Mañosa, and A. Planes. *Nat. Mater.* 4, 450 (2005).
10. I. Škorvánek and J. Kovác. *Czech. J. Phys.* 54 (1), 189 (2004).
11. V. Franco, J.S. Blázquez, C.F. Conde, and A. Conde. *Appl. Phys. Lett.* 88, 042505 (2006).
12. V. Franco, J.M. Borrego, C.F. Conde, and A. Conde. *J. Appl. Phys.* 100, 083903 (2006).
13. J.J. Ipus, J.S. Blázquez, V. Franco, A. Conde, and L.F. Kiss. *J. Appl. Phys.* 105, 123922 (2009).
14. H. Ucar, M. Craven, D.E. Laughlin, and M.E. McHenry. *J. Electron. Mater.* 43, 137 (2014).
15. N.J. Jones, H. Ucar, J.J. Ipus, M.E. McHenry, and D.E. Laughlin. *J. Appl. Phys.* 111, 07A334 (2012).
16. K.A. Gallagher, M.A. Willard, V. Zabenkin, D.E. Laughlin, and M.E. McHenry. *J. Appl. Phys.* 85, 5130 (1999).
17. H. Ucar, J.J. Ipus, D.E. Laughlin, and M.E. McHenry. *J. Appl. Phys.* 113, 17A918 (2013).
18. J.J. Ipus, P. Herre, P.R. Ohodnicki, and M.E. McHenry. *J. Appl. Phys.* 11, 07A323 (2012).
19. J.J. Ipus, H. Ucar, and M.E. McHenry. *IEEE Trans. Magn.* 47, 2494 (2011).
20. F. Körmann, D. Ma, D.D. Belyea, M.S. Lucas, C.W. Miller, B. Grabowski, M.H.F. Sluiter. *Appl. Phys. Lett.* 107, 142404 (2015).
21. D. Maa, B. Grabowski, F. Körmannb, J. Neugebauer, and D. Raabe. *Acta Mater.* 100, 90 (2015).
22. A. Bensadiq, H. Zaari, A. Benyoussef, and A.E. Kenz. *J. Solid State Chem.* 241, 38 (2016).
23. M.S. Lucas, D. Belyea, C. Bauer, N. Bryant, E. Michel, Z. Turgut, S.O. Leontsev, J. Horward, S.L. Semiatin, M.E. McHenry, and C.W. Miller. *J. Appl. Phys.* 113, 17A923 (2013).
24. M.E. McHenry and M. Lucas, *Characterization of Materials*, second-edn. (Wiley, New York, 2012), pp. 1–12.
25. H. Ucar. Carnegie Mellon University, Pittsburgh, PA. Unpublished doctoral dissertation (2013).
26. J.W. Yeh, Y.L. Chen, S.J. Lin, and S.K. *Chen. Mater. Sci. Forum* 560, 1 (2007).
27. J.-W. Yeh. *Ann. Chim.* 31, 633 (2006).
28. J. Yeh, S. Chen, J. Gan, S. Lin, T. Chin, T. Shun, C. Tsau, and S. Chang. *Metall. Mater. Trans. A* 35A, 2533 (2004).
29. U. Dahlborg, J. Cornide, M. Calvo-Dahlborg, T. Hansen, A. Fitch, Z. Leong, S. Chambreland, and R. Goodall. *J. Alloys Compd.* 681, 330 (2016).
30. F. He, Z. Wang, Q. Wu, J. Li, J. Wang, and C. Liu. *Scr. Mater.* 126, 15 (2017).
31. J.W. Yeh, S.K. Chen, S.J. Lin, J.Y. Gan, T.S. Chin, T.T. Shun, C.H. Tsau, and S.Y. Chang. *Adv. Eng. Mater.* 6, 299 (2004).
32. D.D. Belyea, M.S. Lucas, E. Michel, J. Horwath, and C.W. Miller. *Sci. Rep.* 5, 1 (2015).
33. M. Kurniawan, A. Perrin, P. Xu, V. Keylin, and M. McHenry. *IEEE Magn. Lett.* 7, 6105005 (2016).
34. J. Nelson and D. Riley. *Proc. Phys. Soc.* 57, 160 (1945).
35. K. Engelbrecht, C.R.H. Bahl, and K.K. Nielsen. *Int. J. Refrig.* 34, 1132 (2011).
36. U. Gonser. Mossbauer Spectroscopy, Topics in Applied Physics Series, (Springer, Berlin, 1975).